

Journal of Rehabilitation in Civil Engineering

Journal homepage: https://civiljournal.semnan.ac.ir/

Evaluation of Ductility Capacity of the Two Existing Joglo Timber Buildings

Yosafat Aji Pranata 1,*

- 1. Professor, Master Program in Civil Engineering, Maranatha Christian University, Indonesia
- * Corresponding author: yosafat.ap@eng.maranatha.edu

ARTICLE INFO

Article history:

Received: 18 April 2025 Revised: 03 August 2025 Accepted: 17 August 2025

Keywords: Ductility capacity; Capacity curve; Joglo; Timber building; Earthquake.

ABSTRACT

This study aimed to develop a 3D model of existing timber buildings to obtain the capacity curve and ductility capacity of structural systems under lateral loads. The research scope involved a case study of two existing Joglo timber buildings. Nonlinear modeling of beams and columns was performed using hinge property data for each member. Joint modeling employed spring elements to account for the effect of rotational stiffness. The evaluations included the capacity curve, ductility capacity, plastic hinge mechanisms, and energy dissipation. Results from the pushover analysis produced a capacity curve used to investigate ductility capacity and energy dissipation. Structural performance in y-directions exhibited both the xand similar behavior. characterized as partially ductile. The existing timber buildings demonstrated ductility capacities ranging from 2.36 placing them in the partial ductility category. These results meet the building criteria for earthquake zones with a peak ground acceleration (PGA) exceeding 0.10g. The plastic hinge mechanism the strong column-weak beam criterion. The satisfied displacements at the Collapse Prevention level were 137.36 mm (Joglo-M) and 139.03 mm (Joglo-N). These values indicate that the post-elastic behavior of the structures exceeds the permitted limits, suggesting good energy dissipation capacity before final failure. Notably, buildings these two have withstanding several earthquakes over the past twenty years without sustaining damage.

E-ISSN: 2345-4423

© 2025 The Authors. Journal of Rehabilitation in Civil Engineering published by Semnan University Press. This is an open access article under the CC-BY 4.0 license. (https://creativecommons.org/licenses/by/4.0/)

How to cite this article:

Pranata, Y. Aji (2026). Evaluation of Ductility Capacity of the Two Existing Joglo Timber Buildings. Journal of Rehabilitation in Civil Engineering, 14(2), 2317 https://doi.org/10.22075/jrce.2025.2317

1. Introduction

Collapse analysis in timber structures involves assessing their potential for failure, often using methods such as numerical simulations or experimental testing, to understand failure mechanisms and ensure structural robustness. The performance-based design method is a seismic design approach that focuses on the expected performance and displacement of a structure. Pushover analysis, as a performance-based analysis technique, can be used to evaluate moment-resisting frame system buildings [1,2]. In its development, pushover analysis has been combined with the capacity spectrum method [3], including the proposal of a new approach for calculating capacity curves and determining performance points.

Timber-frame structures are the most commonly used structural form in single-story and low-rise residential buildings. These structures perform well in terms of life safety (LS) and collapse prevention (CP) levels during major earthquakes [4]. In 2006, a strong earthquake struck Yogyakarta [5] causing damage and failure in many multi-story buildings. However, traditional wooden buildings generally did not sustain damage to their structural members.

The research question is: How did the Joglo building avoid damage during a strong earthquake? The hypothesis is that the non-rigid connection system influences stiffness behavior (ductility capacity) and energy dissipation, thereby reducing the earthquake forces transmitted to the structural system. Additionally, the quality of the wood used for the beams and columns affects the building's strength.

This study aimed to develop a 3D model of existing timber buildings to obtain the capacity curve and ductility capacity of structural systems under lateral loads.

The scope of this research is a case study involving two existing Joglo timber buildings. The structures are modeled as frame elements consisting of beams, columns, roof beams, and lateral bracing members. The mechanical properties of the wood are based on data from previous research [6]. Structural modeling is performed using software based on the finite element method [7]. Nonlinear modeling of beam and column members is conducted using hinge property data for each member [7]. The modeling of beam-to-main column and beam-to-side column joints employs spring elements to account for the rotational stiffness effects in the connection system [8,9]. The evaluation in this study includes the capacity curve, ductility capacity, plastic hinge mechanisms, and energy dissipation (represented by the area under the structure's capacity curve).

The novelty of this research lies in the valuable combination of experimental testing to determine the mechanical properties of structural members and numerical methods to analyze the structural behavior of existing timber buildings under lateral loads. This integrated approach can also be applied in the design of new wooden buildings to ensure that the structure performs safely during strong earthquakes.

There are many traditional wooden structures in Southeast Asia that are considered highly valuable assets due to their strong cultural significance and local knowledge [10]. Research on timber structures subjected to gravity and lateral loads has been conducted by Lyu et al. [11]. The behaviors studied included the degradation of strength and stiffness caused by deterioration and damage to these timber structures. The research employed dynamic analysis to examine the dynamic behavior of wooden buildings. Studies investigating existing wooden buildings and the resulting reduction in strength have also been carried out, including an investigation into defects found in historic wooden houses with high cultural significance [12].

Zhang et al. [13] employed finite element models and analysis to study the dynamic characteristics and seismic responses of multi-storey timber structures, using case studies of traditional Chinese buildings. Their simulation utilized spring elements to represent the slip behavior between columns positioned atop base stones. Finite element analysis can also be used to model the failure processes of timber structural

members. Vodiannikov et al. conducted numerical analyses and experimental tests to investigate the failure mechanisms of glued laminated timber beams [14].

Research on the strength and stiffness behavior of multi-storey wooden buildings has been conducted by Li and Lam [15]. Additionally, a case study of mass timber buildings [16] includes an analysis of a six-story medium-rise building in Japan affected by the Kobe earthquake [17]. This study involved dynamic modeling to investigate the collapse behavior of 3D wooden buildings. Collapse is characterized by a chain reaction of failures, accompanied by large displacements and the inelastic behavior of materials and structural elements. A model capable of collapse analysis can support risk-informed decision-making to enhance building safety [17–19].

A study investigating the causes of the collapses of two timber sheds located in Poland was conducted by Szczotka [20], which included recommendations and technical solutions for their repair. Additionally, a study on the seismic performance of wood-frame buildings in India was carried out using pushover analysis to examine their nonlinear behavior [21].

Kiyono and Furukawa [22] conducted research to model the collapse of timber-frame houses during earthquakes using the distinct element method (DEM). This method simulates the collapse process of timber-frame structures under dynamic loading. The timber-frame structure is modeled using distinct element types connected by springs and dashpots to represent contact between members. Additionally, Yu and Takeuchi [23] performed simulations of seismic and SAR images on a 3D model of a typical Japanese wooden building using collapse analysis.

2. Theoretical background

2.1. Ductility class of the structures

Ductility is defined as the ability of a structure to sustain large displacements beyond its elastic behavior without failure. Ductility (μ) is expressed in terms of demand, representing the maximum ductility level that the structure can reach during seismic activity. This demand depends on both the structural capacity and the earthquake loads.

Structures with frame systems can be categorized into ductility classes based on their energy dissipation capacity [24,25]. These classes include low ductility, which does not require delayed ductility and achieves seismic resistance through the structure's inherent capacity (μ = 1.5); medium ductility, which allows for higher levels of ductility and corresponds to responsive design demands (μ ranging from 1.5 to 4); and high ductility, which permits even greater ductility levels and addresses strict and complex design requirements (μ > 4). The low ductility class (DCL) is designed for seismic loading based on a design seismic event with a return period of 475 years and is limited to regions where the maximum ground design acceleration is less than 0.10g. In areas with medium or high seismic activity, buildings must be designed with a higher ductility class.

2.2. Performance-based seismic design for timber buildings

Research and development of performance-based seismic design for timber buildings, particularly those with frame structural systems, have been ongoing since the early 2000s. This effort began with Filiatrault's study [26] on performance-based seismic design for timber frame structures, followed by Jain et al.'s research [27] on pushover analysis of timber frame buildings. Subsequent work includes Lindt et al.'s study [28] on performance-based seismic design for timber frame structures and Tesfamariam's research [29] on performance-based seismic design for tall timber buildings. Several design codes for wooden construction, including NDS [30], SNI 7973 [31], and Eurocode 5 [32], regulate the technical design of cross-sectional and connection capacities. However, these codes do not specifically address displacement-based design for building structures.

To study the strength and stiffness (ductility capacity) of a building, it is essential to obtain a capacity curve that represents the building's structural condition. This capacity curve can be derived through nonlinear static analysis, such as pushover analysis. Pushover analysis is a structural engineering method used to evaluate a structure's seismic performance by simulating a gradual increase in lateral static loads. This analysis helps determine the structure's capacity and behavior under extreme loading, providing a clearer understanding of its performance and potential failure mechanisms.

2.3. Acceptance criteria

Performance-based seismic design employs the concept of categorizing buildings into multiple performance levels based on their capacity curves. Figure 1 illustrates the capacity curve, which represents the relationship between force and displacement and is used to define structural performance criteria according to the FEMA 356 standard [33]. FEMA 356 establishes acceptance criteria for seismic rehabilitation, focusing on three performance levels: Immediate Occupancy (IO), Life Safety (LS), and Collapse Prevention (CP).

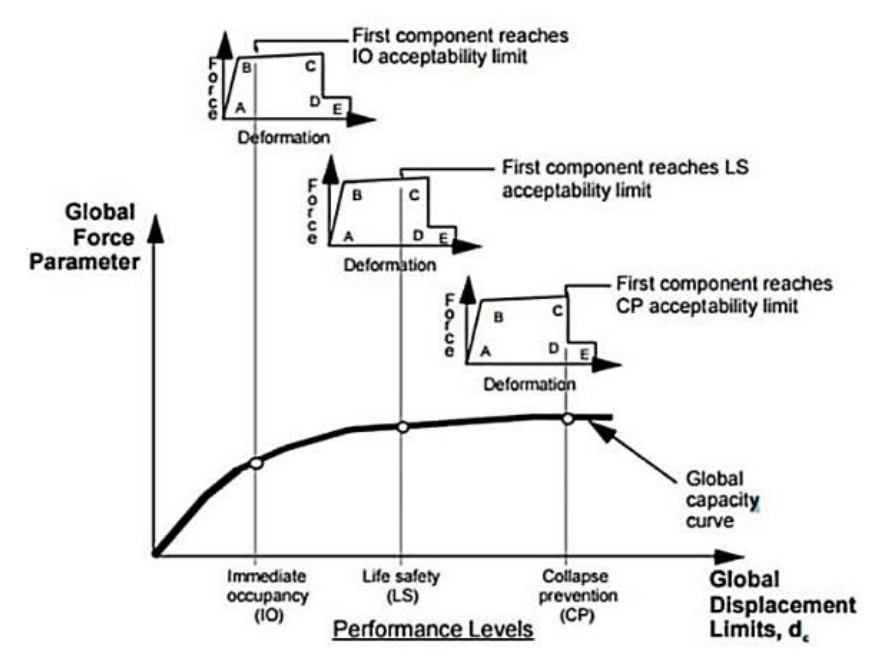


Fig. 1. Building performance acceptance criteria [33].

These criteria are based on factors such as displacement and drift (limits on the amount of deformation or lateral movement a building can experience), strength and stiffness (minimum strength and stiffness requirements for structural elements), and damage state (acceptable levels of damage to structural and non-structural components). At the Immediate Occupancy (IO) level, minor failures may occur in non-structural components, while structural elements remain intact. The structure remains functional with minimal damage, ensuring occupants can continue to use it safely.

At the Life Safety (LS) level, only limited damage is observed, and occupant safety is ensured. The stiffness and rigidity of the main beam, side beam, main column, and side column members are maintained. Structural collapse is prevented, safeguarding occupants during and after an earthquake. At the Collapse Prevention (CP) level, some structural members may fail, and permanent displacements occur; however, overall structural collapse is still prevented, even under severe earthquake conditions.

2.4. Rotation stiffness

Three-dimensional analysis of wooden buildings, which are framed structural systems, requires modeling beam elements, column elements, and their connections to accurately represent existing wooden

structures. The mechanical properties of beam and column elements can be determined through non-destructive testing [34]. To characterize the behavior of timber connections, this research employs a spring element approach [8,9] to model the rotational stiffness (r). Equations 1 and 2 present empirical values of rotational stiffness (r_1 and r_2) for two types of timber connections. Figure 2a illustrates type 1 connections as proposed by Fang et al. [9], while Figure 2b illustrates type 2 connections as proposed by Moradei et al. [8].

$$r_1 = 12.5 \text{ kN.m}$$
 (1)



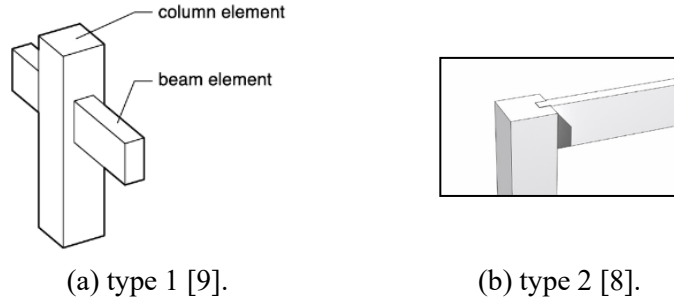


Fig. 2. Schematic beam to column joints for reference of rotational stiffness.

3. Methods

The research method employed in this study is the performance-based seismic design approach, utilizing pushover analysis. A three-dimensional structural model was developed using SAP2000, a finite element-based software [7]. Two existing Joglo timber buildings serve as case studies. These buildings feature a unique column placement concept, with four main columns positioned at the center of the structure's mass. The main columns differ in height from the side columns. The four main columns are connected by four primary beams. At a lower elevation, four wooden beams function as bracing. Similarly, the side columns are connected by side beams, with wooden beams at a lower elevation serving as bracing.

These two existing buildings are located in the Maguwo District (hereinafter referred to as Joglo-M) and Nogotirto District (hereinafter referred to as Joglo-N). Both locations are situated in Sleman Regency, Special Region of Yogyakarta Province, Indonesia. The Joglo-M building is positioned at latitude -7.7731 and longitude 110.4351. According to the earthquake spectral response map [35], it has a Peak Ground Acceleration (PGA) of 0.53g. Meanwhile, the Joglo-N building is located at latitude -7.7650 and longitude 110.3366 and has a PGA of 0.46g based on the same map [35].

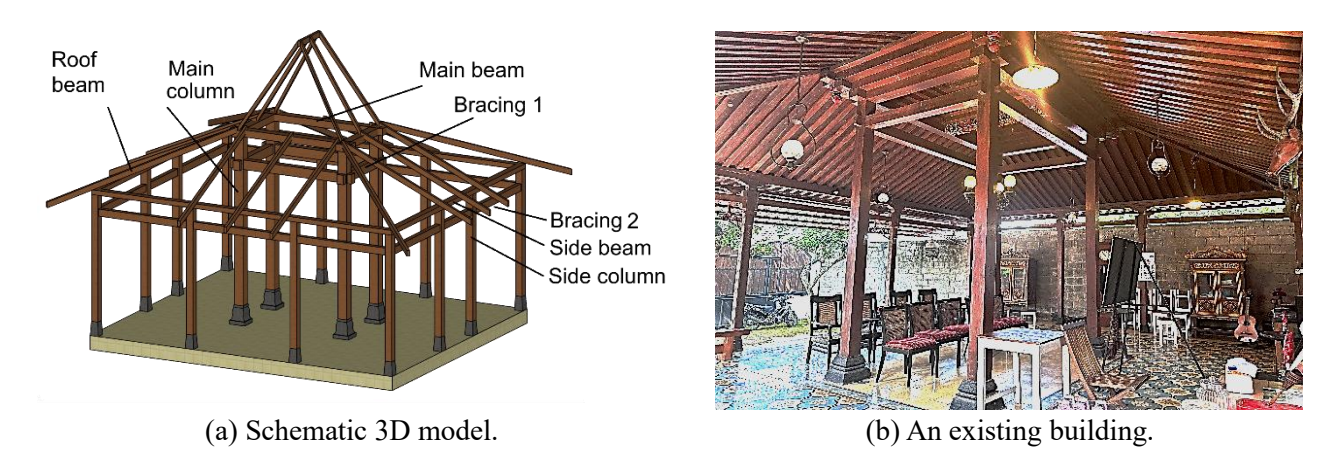
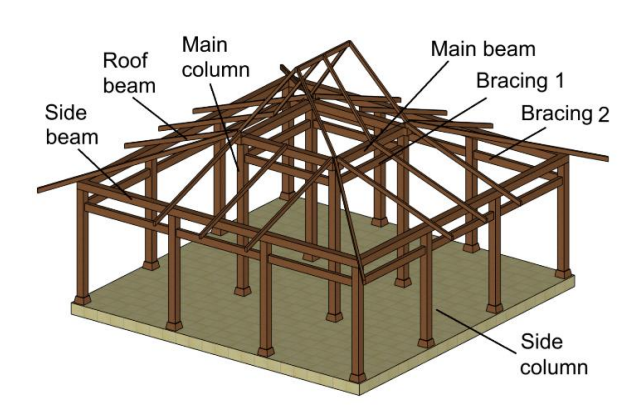


Fig. 3. The existing Joglo-M timber building.





(a) Schematic 3D model.

(b) An existing building.

Fig. 4. The existing Joglo-N timber building.

Table 1. Dimensions and size of cross-section of beams and columns [36].

		LJ
Dimension of member	Joglo-M	Joglo-N
Main beam	150mm x 200mm	200mm x 200mm
Side beam	120mm x 120mm	150mm x 150mm
Bracing 1	100mm x 150mm	150mm x 200mm
Bracing 2	50mm x 120mm	100mm x 150mm
Roof beam	100mm x 100mm	100mm x 100mm
Main column	150mm x 150mm	200mm x 200mm
Side column	120mm x 120mm	150mm x 150mm

Figure 3a and Figure 4a present the schematic 3D models of the existing Joglo-M and Joglo-N structures. Figure 3b depicts the existing Joglo-M timber building, which measures 6.8 m by 5.8 m, with a building area of 39.44 m². The height of the center column is 4.15 m, while the edge column is 3 m. The total height of Joglo-M, measured at the top roof elevation, is 6.15 m. Figure 4b shows the existing Joglo-N timber building, which measures 8.4 m by 8.4 m, with a building area of 70.56 m². The height of the center column is 4.50 m, while the edge column is 3 m. The total height of Joglo-N, at the top roof elevation, is 7.00 m.

The dimensions and sizes of the beam and column cross-sections for the Joglo-M and Joglo-N are presented in Table 1. Figure 5 illustrates the beam-to-column joint and beam-to-beam connection of the existing Joglo-M timber building, while Figure 6 depicts the beam-to-column and beam-to-beam joints of the existing Joglo-N timber building. The main beam and main column joint connection system functions as a moment-resistant frame because the wooden structure's rigidity and stability are achieved through the locking joint between the main column and main beam [37–39].

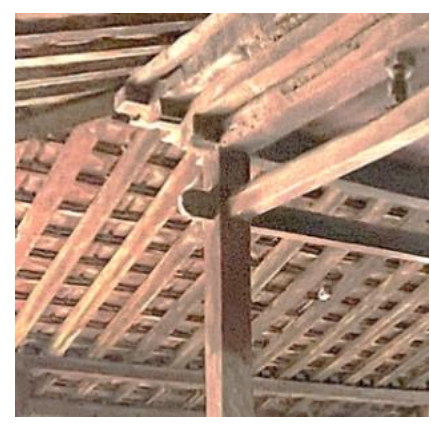


(a) Beam-to-main column joint.



(b) beam-to-side column joint.

Fig. 5. Beam-to-column joints in Joglo-M building.





(a) Beam-to-main column joint.

(b) beam-to-side column joint.

Fig. 6. Beam-to-column joints in Joglo-N building.

Table 2. The mechanical properties of timber on existing buildings [36].

Existing building	Modulus of elasticity (MPa)	Specific gravity
Joglo-M	18526.09	0.80
Joglo-N	21483.90	0.80

The mechanical properties of wood, as shown in Table 2, were obtained through non-destructive testing on samples from the main and side columns, main and side beams, bracing, and roof beams [36]. For the Joglo-M building, samples were taken from 18 members (beams and columns). The test involved measuring at nine points each at the support and mid-span of each member, totaling 475 test points. The Joglo-N building test included samples from 10 members, with a total of 268 test points. According to information from the homeowner, the existing Joglo-N building is older and was constructed before the Joglo-M building. The non-destructive test is based on the concept of wave propagation velocity measurement [34] and utilizes two transducers. One transducer acts as the transmitter, and the other serves as the receiver of ultrasonic wave signals. These signals are then measured and converted into velocity to calculate the dynamic modulus of elasticity, which correlates with the static modulus of elasticity [40,41].

Structural modeling is performed using software based on the finite element method [7], where the nonlinear behavior of beam and column members is represented through hinge property data for each member. Beam-to-main column and beam-to-side column joints are modeled using spring elements to account for the rotational stiffness effects within the connection system [8,9]. The Joglo building features columns resting on the foundation, which act as pin supports—resisting horizontal and vertical translation but not moments. Material properties are modeled using empirical data obtained from previous studies on similar existing buildings [36], as summarized in Table 2. According to the NDS 2024 [30] and SNI 7973:2013 [31] codes, the wood used in the existing Joglo-M building is classified as strength class E18, while the wood in the Joglo-N building falls under strength class E21. The Joglo building features columns resting on the foundation that function as pin supports, meaning they do not resist moments but prevent translations. Figure 7a shows a schematic of the 3D model of Joglo-M, while Figure 7b presents the schematic of the 3D model of Joglo-N. Gravity loads, including the self-weight of the roof structure and tiles, as well as live loads in accordance with SNI 1727 codes [42], are modeled as concentrated loads applied to the upper ends of the columns.



Fig. 7. Schematic 3D model of the existing buildings.

4. Results and discussion

The magnitude of the load was calculated based on the tributary area principle. Dead load and live load models are shown in Figure 8a (dead loads) and Figure 8b (live loads) for Joglo-M, while those for Joglo-N are shown in Figure 9a (dead loads) and Figure 9b (live loads). The structural performance was evaluated using pushover analysis by applying lateral loads with increments of 1 kN until the building collapsed. Following the displacement-based design method, the target displacement was set at 150 mm to obtain the capacity curve and assess the post-elastic structural behavior.

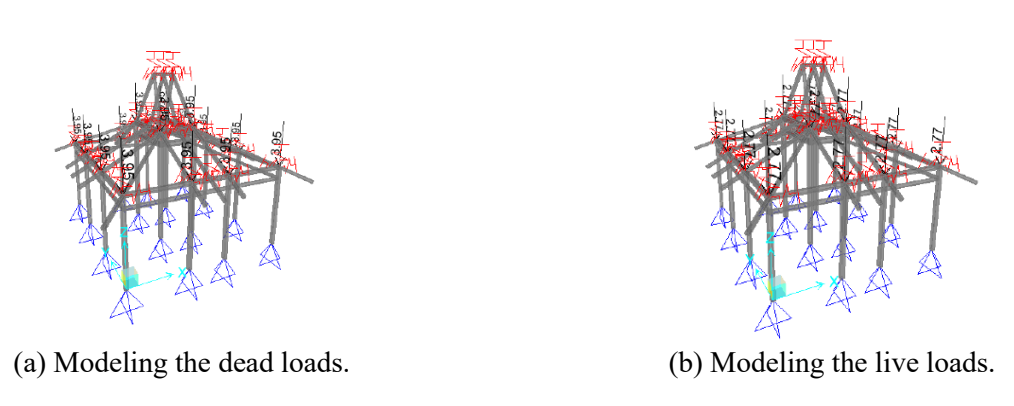


Fig. 8. Modeling loads on Joglo-M (unit in kN).

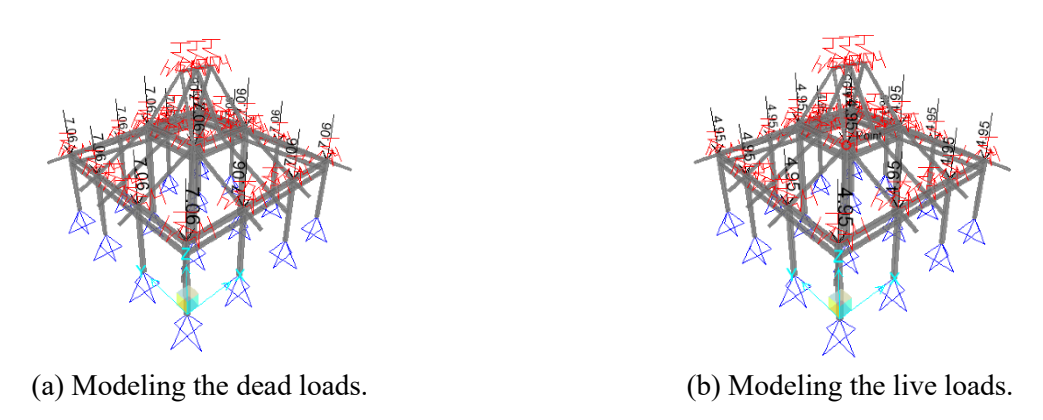


Fig. 9. Modeling loads on Joglo-N (unit in kN).

The load pattern used in the analysis consisted of a concentrated load applied to eight joints of the columns and beams at an elevation of +3 meters. The analysis results are presented in Figures 10 and 11 for the Joglo-M building, and Figures 12 and 13 for the Joglo-N building.

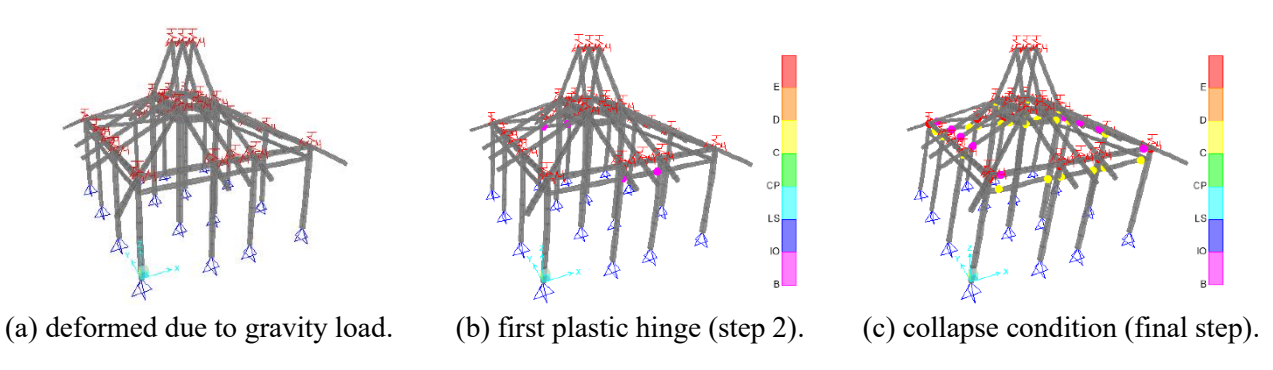


Fig. 10. The mechanism of plastic hinge formation in Joglo-M buildings: pushover load in the x-direction.

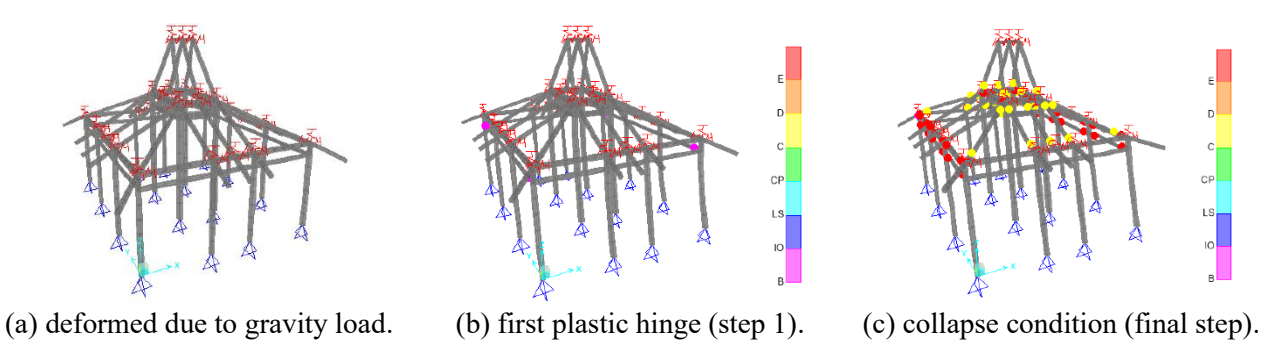


Fig. 11. The mechanism of plastic hinge formation in Joglo-M buildings: pushover load in the y-direction.

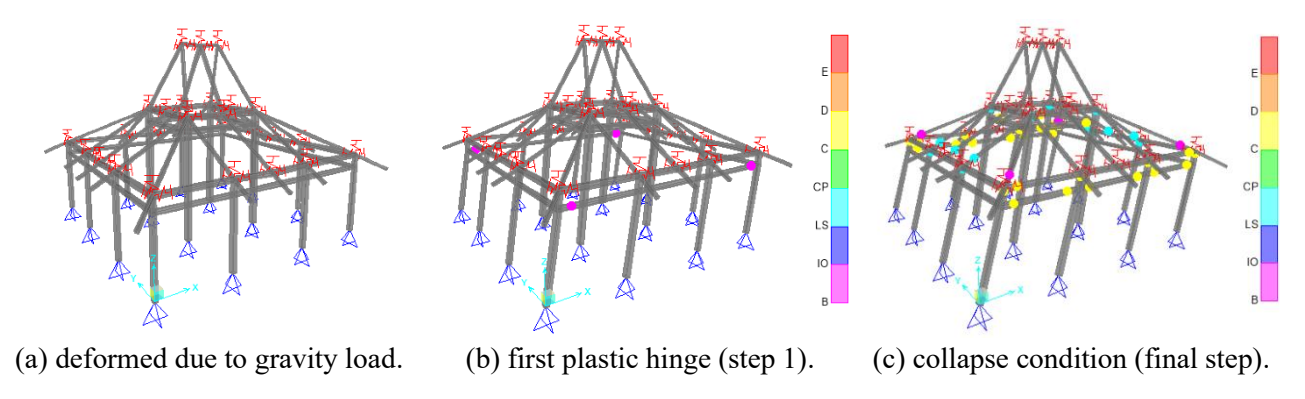


Fig. 12. The mechanism of plastic hinge formation in Joglo-N buildings: pushover load in the x-direction.

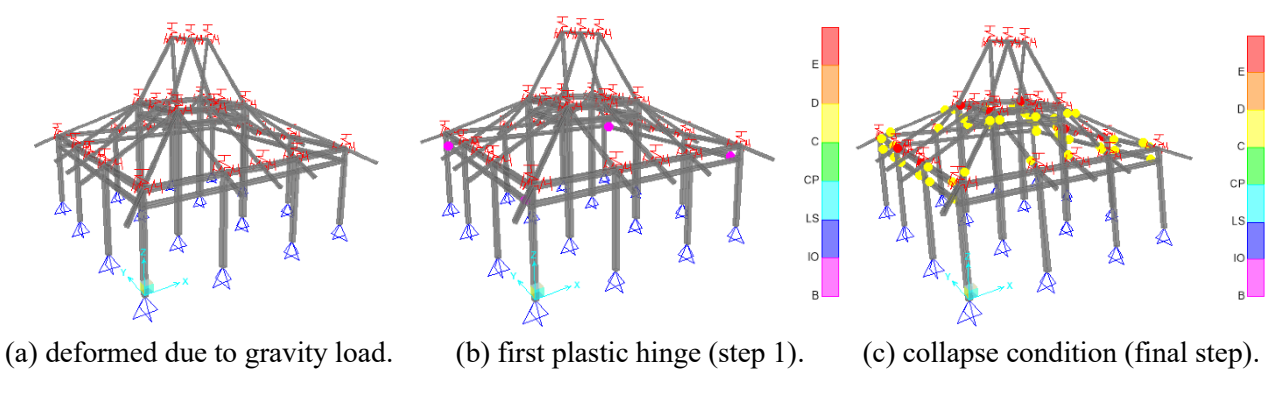
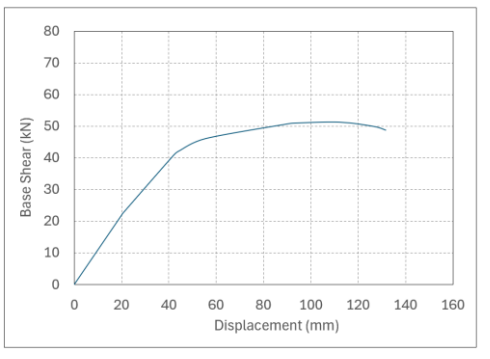
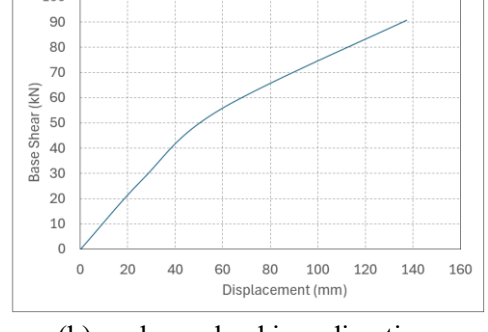


Fig. 13. The mechanism of plastic hinge formation in Joglo-N buildings: pushover load in the y-direction.

The evaluation includes the structural capacity curve, structural ductility capacity, and the mechanisms of plastic hinge formation and damage states. The results of the pushover analysis of the Joglo-M building,

subjected to a pushover load in the x-direction (Figure 10), show that plastic hinges first develop in the side beam. Furthermore, as the lateral load gradually increases, plastic hinges form in additional beams and columns. Similarly, the lateral pushover load applied in the y-direction (Figure 11) exhibits the same pattern in the formation of plastic hinges. The pushover analysis results for the Joglo-N building, with loads applied in the x-direction (Figure 12) and y-direction (Figure 13), generally follow the same trend observed in the Joglo-M building. Therefore, it can be concluded that a strong column—weak beam mechanism is present.

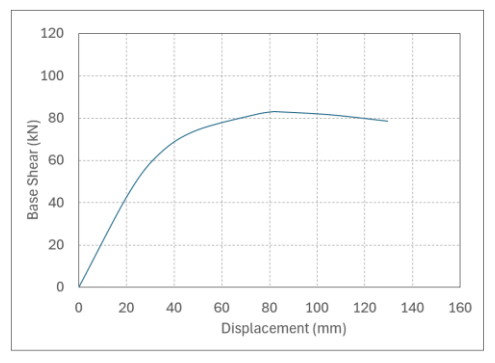




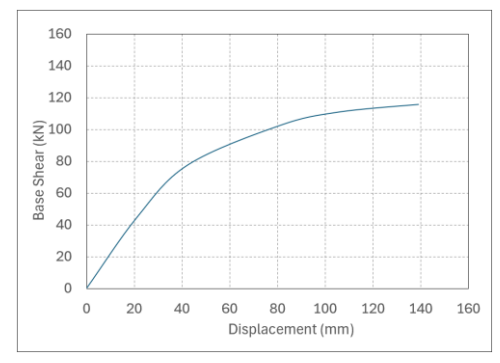
(a) pushover load in x-direction.

(b) pushover load in y-direction.

Fig. 14. Results obtained from analysis: capacity curve of the Joglo-M building.



(a) pushover load in x-direction.



(b) pushover load in y-direction.

Fig. 15. Results obtained from analysis: capacity curve of the Joglo-N building.

The capacity curve of the Joglo-M, shown in Figure 14, exhibits a bilinear trend for both the x- and y-directions. However, the structural behavior differs after reaching the peak load. Specifically, in the x-direction, there is a reduction in strength following the peak load, whereas in the y-direction, the strength remains stable. This difference is likely due to the varying stiffness of the Joglo roof structure along the two main axes. The capacity curve of the Joglo-N, shown in Figure 15, generally follows the same trend as that of the Joglo-M. This similarity arises because both buildings share the same column configuration.

Table 3. Results obtained from calculation: the ductility capacity of the Joglo-M and Joglo-N buildings.

Building	Pushover Load	$P_{y}(kN)$	$D_{y}(kN)$	$P_{u}(kN)$	D _u (mm)	μ
Joglo-M	x-direction	41.07	42.21	51.37	112.04	2.65
	y-direction	55.09	58.25	90.82	137.36	2.36
Joglo-N	x-direction	63.10	33.81	83.07	82.30	2.43
	y-direction	77.71	42.38	115.86	139.03	3.28

 P_y defines the base shear at the proportional or yield point, Pu defines the base shear at the ultimate point, D_y represents the displacement when P_y is reached, D_u represents the displacement when P_u is reached,

and μ denotes the ductility capacity. The results of the study on the building capacity curve, as shown in Table 3, indicate that the ductility capacity (μ) of the Joglo-M building ranges from 2.36 to 2.65 (based on pushover loads in both directions along the main axis of the building). For the Joglo-N building, the study results shown in Table 3 reveal that the ductility capacity ranges from 2.43 to 3.28. These findings suggest that the ductility capacities of both buildings fall within the partial ductility criteria according to EN 8 [24,25] and SNI 1726 [43]. Buildings with partial ductility levels can meet the requirements for moderate to severe earthquake zones with a peak ground acceleration (PGA) exceeding 0.10g.

The capacity curve presents the results of the investigation, indicating that the Joglo-M building exhibited a behavioral change from elastic to plastic (proportional or yield point) when the displacement (D_y) reached 42.21 mm in the x-direction and 58.25 mm in the y-direction of the pushover load.

Based on the earthquake code SNI 1726 [43], these values have not exceeded the permissible limit (Δ_a), which is 0.02 times the building's elevation height, or 0.02 × 4150 mm = 83 mm. The ratio of the proportional displacement to the displacement limit (P_y/Δ_a) is 42.21/83 = 0.51 (x-direction) and 58.25/83 = 0.71 (y-direction). For the Joglo-N building, the proportional or yield displacement (D_y) is 33.81 mm (x-direction) and 42.38 mm (y-direction). These values also do not exceed the permissible limit, which is 0.02×4500 mm = 90 mm. The ratio of the proportional displacement to the displacement limit (P_y/Δ_a) is 33.81/90 = 0.36 (x-direction) and 42.38/90 = 0.47 (y-direction). These results indicate that the capacity curve provides structural behavior data within the elastic range, as the displacement ratios are below the permissible limit ($P_y/\Delta_a < 1.0$). Considering that the existing building has not experienced damage to structural elements or permanent lateral displacement during several previous strong earthquakes, it remains within the elastic behavior range.

Table 4. The damage state of the Joglo-M building due to pushover loads.

		<u> </u>		
Direction	Pushover Load	IO	LS	СР
x-direction	Base Shear (kN)	22.58	41.07	46.18
x-direction	Displacement (mm)	20.59	42.21	55.54
y-direction	Base Shear (kN)	27.81	55.09	90.82
	Displacement (mm)	26.21	58.25	137.36

Table 5. The damage state of the Joglo-N building due to pushover loads.

Direction	Pushover Load	IO	LS	CP
x-direction	Base Shear (kN)	44.54	74.06	81.76
	Displacement (mm)	21.02	49.00	74.34
y-direction	Base Shear (kN)	44.54	77.71	115.86
	Displacement (mm)	21.02	42.38	139.03

The damage state investigation was conducted by examining the mechanism of plastic hinge formation. The results, presented in Table 4 for the Joglo-M building and Table 5 for the Joglo-N building, show that when the structures reach their capacity at the LS level, the maximum displacement of Joglo-M is 58.25 mm, which does not exceed the allowable limit of 83 mm, resulting in a ratio of 58.25/83 = 0.71. Similarly, the maximum displacement for Joglo-N is 49 mm, which also remains below the allowable limit of 90 mm, with a ratio of 49/90 = 0.54. These findings indicate that both buildings maintain adequate stiffness and rigidity, preserving the integrity of the main members of the existing timber structures.

As shown in Tables 4 and 5, the peak displacement of the Joglo-M at the CP level is 137.36 mm, while for the Joglo-N, it is 139.03 mm. The CP level condition occurs when the building's displacement exceeds the allowable limits of 83 mm for Joglo-M and 90 mm for Joglo-N. These values indicate that the post-

elastic behavior of the structures extends beyond the permitted limits. This suggests that the structures exhibit good energy dissipation before the final failure, which occurs at the peak base shear on the capacity curve. This allowable limit can serve as a conservative reference in building design.

Table 6. Results obtained from calculation: the initial stiffness and energy dissipation (area of the capacity curve).

Buildings	Pushover Load	The initial stiffness (kN/mm)	Energy dissipation (J)
Joglo-M	x-direction	1.03	5288.25
	y-direction	1.06	7463.47
Joglo-N	x-direction	0.54	8656.80
	y-direction	0.55	11677.33

Table 6 presents the results of the initial stiffness, indicated by the slope in the elastic range of the capacity curve, and the area under the capacity curve, which relates to the potential energy dissipation in these buildings. The investigation results show that the initial stiffness of the capacity curve in both the x-and y-directions is nearly identical. This similarity can be attributed to the design of the joglo building plan, which is almost symmetrical, with the only difference being the rooftop configuration. It is well established that symmetrical buildings perform better than asymmetrical ones during earthquakes [44]. However, the area under the capacity curve obtained from the analysis with the y-direction pushover load is greater than that of the x-direction. This parameter is valuable for further studies on energy dissipation. The purpose of energy dissipation is to reduce the intensity of vibrations and deformations, thereby preventing excessive damage to the building's core structure. By absorbing earthquake energy, energy dissipation systems help maintain the structural integrity of buildings, even during strong ground shaking.

The quality of the wood classified as E18 strength class for the Joglo-M and E21 for the Joglo-N used for the main structural members, along with the non-rigid connection models, affects the strength and stiffness behavior of the building. However, the primary focus of investigation has been the structural system of the Joglo building. The core of the structure lies in the section where the four main beams support the four main columns, located at the center of the building. This structural system provides the building with stiffness and features a symmetrical plan layout, which enhances resistance to lateral loads.

5. Conclusions

The pushover analysis of the existing timber buildings, conducted using the 3D numerical model developed in this research, produces a capacity curve that characterizes the building's structural performance. This curve is used to evaluate ductility capacity and energy dissipation. The capacity curves obtained from pushover loads applied in both the x- and y-directions exhibit similar behavior, indicating partial ductility for both the existing Joglo-M and Joglo-N buildings. The curves follow a bilinear pattern, consisting of an elastic range, a post-elastic range, and terminating at the peak or failure point. The ductility capacity of the Joglo-M and Joglo-N buildings ranges from 2.36 to 3.28, placing them within the partial ductility category. These buildings are located in areas with peak ground accelerations (PGA) of 0.53g (Joglo-M) and 0.46g (Joglo-N). The measured ductility capacities satisfy the building criteria for moderate to severe earthquake zones, which require a PGA exceeding 0.10g. The pushover analysis reveals the plastic hinge mechanism pattern. It shows that the plastic hinge initially forms in the side beam rather than in the column, indicating a strong column-weak beam mechanism. The peak displacement at the Collapse Prevention level is 137.36 mm for Joglo-M and 139.03 mm for Joglo-N. Both values exceed the allowable limits of 83 mm for Joglo-M and 90 mm for Joglo-N. These results suggest that the post-elastic behavior of the structures extends beyond the permitted limits, indicating good energy dissipation capacity before final failure at the peak base shear on the capacity curve. Notably,

both buildings have remained undamaged during several earthquakes in Yogyakarta over the past twenty years, including the significant earthquake in 2006.

This study has several limitations, including the lack of empirical data to model the rotational stiffness of roof structure beams. Additionally, the moment-curvature model is assumed to be the same for all types of wooden beams. Future research should include partial testing of connections on roof beams. Different earthquake loading methods, such as inelastic time-history analysis, could be employed to better understand the inelastic behavior under specific earthquake records. Practical recommendations for future studies include exploring various performance-based design methods to develop more conservative capacity curves.

Funding

This research was funded by Maranatha Christian University for the fiscal year 2025.

Conflicts of interest

The authors declare that they have no known competing financial interests or personal relationships that could have appeared to influence the work reported in this paper.

Authors contribution statement

Yosafat Pranata: Conceptualization; Investigation; Methodology; Project administration; Resources; Validation; Writing – original draft; Writing – review & editing.

References

- [1] Barros RC, Braz-César MT, Naderpour H, Khatami SM. Comparative Review of the Performance Based Design of Building Structures Using Static Non-Linear Analysis, Part A: Steel Braced Frames. J Rehabil Civ Eng 2013;1:24–39. https://doi.org/https://doi.org/10.22075/jrce.2014.214.
- [2] Kheyroddin A, Gholhaki M, Pachideh G. Seismic Evaluation of Reinforced Concrete Moment Frames Retrofitted with Steel Braces Using IDA and Pushover Methods in the Near-Fault Field. J Rehabil Civ Eng 2019;7:159–73. https://doi.org/10.22075/JRCE.2018.12347.1211.
- [3] Golafshar A, Saghafi MH, Eshaghi F. A new method for drawing the capacity spectrum for seismic analysis and structural rehabilitation. J Rehabil Civ Eng 2020;8:109–23. https://doi.org/10.22075/JRCE.2020.19106.1360.
- [4] Gu J. Sensitivity analysis of probabilistic seismic behaviour of wood frame buildings. Earthquakes Struct 2016;11:109–27. https://doi.org/https://doi.org/10.12989/eas.2016.11.1.109.
- [5] Librian V, Ramdhan M, Nugraha AD, Mukti MM, Syuhada S, Luhr BG, et al. Detailed seismic structure beneath the earthquake zone of Yogyakarta 2006 (Mw ~6.4), Indonesia, from local earthquake tomography. Phys Earth Planet Inter 2024;351:107170. https://doi.org/https://doi.org/10.1016/j.pepi.2024.107170.
- [6] Pranata YA, Pattipawaej OC, Setiadi A. Beam-column and beam-beam connections for earthquake-resistant wooden houses. Indonesia: 2024.
- [7] CSI. SAP2000 technical manual notes 2023.
- [8] Moradei J, Brütting J, Fivet C, Sherrow-Groves N, Wilson D, Fischer A, et al. Structural Characterization of Traditional Moment-Resisting Timber Joinery. Proc IASS Symp 2018, Creat Struct Des 2018:8.
- [9] Fang DL, Mueller CT, Brütting J, Fivet C, Moradei J. Rotational stiffness in timber joinery connections: Analytical and experimental characterizations of the nuki joint. Struct Archit Bridg Gap Crossing Borders Proc 4th Int Conf Struct Archit ICSA 2019 2019:229–36. https://doi.org/10.1201/9781315229126-28.
- [10] Wiryomartono B. Traditions and Transformations of Habitation in Indonesia. Springer Singapore; 2020.

- [11] Lyu M, Zhu X, Yang Q. Dynamic field monitoring data analysis of an ancient wooden building in seismic and operational environments. Earthquakes Struct 2016;11:1043–60. https://doi.org/https://doi.org/10.12989/eas.2016.11.6.1043.
- [12] Sodangi M, Kazmi ZA. Seismic Performance of South Nias Traditional Timber Houses: A Priority Ranking Based Condition Assessment. Earthquakes Struct 2020;18:731–42. https://doi.org/https://doi.org/10.12989/eas.2020.18.6.731.
- [13] Zhang X, Ma H, Zhao Y, Zhao H. Dynamic responses on traditional Chinese timber multi-story building with high platform base under earthquake excitations. Earthquakes Struct 2020;19:331–45. https://doi.org/https://doi.org/10.12989/eas.2020.19.5.331.
- [14] Vodiannikov MA, Kashevarova GG, Starobogatov DI. Numerical modeling and full-scale experiments of glued wooden structures joint destruction on carbon-fiber dowel pins. Int J Comput Civ Struct Eng 2020;16:101–12. https://doi.org/10.22337/2587-9618-2020-16-2-101-112.
- [15] Li Y, Lam FCF. Seismic performance of midrise timber structures collapse prevention. Vancouver: 2012.
- [16] Daneshvar H, Chui YH. Disproportionate collapse mitigation in tall mass timber buildings. AB: 2019.
- [17] Cao AS. Modelling progressive collapse of timber buildings and it sapplications. Norwegian University of Science and Technology, 1995.
- [18] Cao AS, Esser L, Glarner B, Frangi A. a Nonlinear Dynamic Model for Collapse Investigations in Tall Timber Buildings Preliminary Results. 13th World Conf Timber Eng WCTE 2023 2023;4:2268–77. https://doi.org/10.52202/069179-0301.
- [19] Cao AS, Esser L, Frangi A. Modelling progressive collapse of timber buildings. Structures 2024;62:106279. https://doi.org/10.1016/j.istruc.2024.106279.
- [20] Szczotka J. The analysis of the causes of the collapse of two timber sheds during the construction. MATEC Web Conf 2019;284:02009. https://doi.org/10.1051/matecconf/201928402009.
- [21] Ghosh S, Chakraborty S. Seismic fragility analysis of wood frame building in hilly region. Earthquakes Struct 2021;20:97–107. https://doi.org/https://doi.org/10.12989/eas.2021.20.1.097.
- [22] Kiyono J, Furukawa A. Casualty occurrence mechanism in the collapse of timber-frame houses during an earthquake. Earthq Eng Struct Dyn 2004;33:1233–48. https://doi.org/10.1002/eqe.402.
- [23] Yu Y, Takeuchi W. Analysis of Scattering Mechanisms in SAR Image Simulations of Japanese Wooden Buildings Damaged by Earthquake. Buildings 2024;14. https://doi.org/10.3390/buildings14113585.
- [24] Eurocode. EN 1998-1:2004 Eurocode 8: Design of structures for earthquake resistance Part 1: General rules, seismic actions and rules for buildings. Ispra: 2004.
- [25] Eurocode. EN 1998-3:2005 Eurocode 8: Design of structures for earthquake resistance Part 3: Assessment and retrofitting of buildings. Ispra: 2005.
- [26] Filiatrault A, Folz B. Performance-Based Seismic Design of Wood Framed Buildings. J Struct Eng 2002;128. https://doi.org/https://doi.org/10.1061/(ASCE)0733-9445(2002)128:1(39).
- [27] Jain A, Hart GC, Ekwueme C, Dumortier AP. Performance Based Pushover Analysis. Proc 13th World Conf Earthq Eng 2004:1–11.
- [28] Lindt JW, Pei S, Liu H. Performance-Based Seismic Design of Wood Frame Buildings Using a Probabilistic System Identification Concept. J Struct Eng 2008;134. https://doi.org/https://doi.org/10.1061/(ASCE)0733-9445(2008)134:2(24.
- [29] Tesfamariam S. Performance-Based Design of Tall Timber Buildings Under Earthquake and Wind Multi-Hazard Loads: Past, Present, and Future. Front Built Environ 2022;8:1–17. https://doi.org/10.3389/fbuil.2022.848698.
- [30] AWC. The 2024 National Design Specification (NDS) for wood construction. Wood Design Standards Committee; 2024.
- [31] NSA. SNI 7973 Design specifications for wood construction. National Standardization Agency; 2013.
- [32] Eurocode. Eurocode 5. EN 1995-1-1:2004 Eurocode 5: Design of timber structures. Ispra: 2004.
- [33] BSSC. NEHRP Recommended seismic provisions for new buildings and other structures volume I FEMA 356. Washington DC: Building Seismic Safety Council; 2020.
- [34] CBS-CBT. Sylvatest 4 user guide. Saint-Sulpice: Concept Bois Technologie; 2023.

- [35] PusGeN. Design of Indonesian spectra. Bandung: PuSGeN Ditjen Cipta Karya Ministry of Public Work and Human Settlement; 2021.
- [36] Pranata YA, Pattipawaej OC, Setiadi A. A. Compression and bearing behavior of teak wood (tectona grandis) for column and connections components of earthquake resistant wooden buildings. Final Report Internal Research Collaboration Scheme with Domestic Partners, Maranatha Christian University; n.d.
- [37] Frick H. Structural patterns and building techniques in Indonesia. Kanisius; 1997.
- [38] Bisatya W. M, Pamuda P. SANTEN-fuse AS ANEARTHQUAKE DAMPER FOR PENDOPO JOGLO. Dimens (Journal Archit Built Environ 2015;42:1–8. https://doi.org/10.9744/dimensi.42.1.1-8.
- [39] Pranata YA, Setiadi A, Suryoatmono B, Novi. Seismic Behavior of Joglo Traditional Wooden House Located in Special Region of Yogyakarta, Indonesia. Civ Eng Archit 2025;13:1171–80. https://doi.org/10.13189/cea.2025.130232.
- [40] Arriaga F, Osuna-Sequera C, Bobadilla I, Esteban M. Prediction of the mechanical properties of timber members in existing structures using the dynamic modulus of elasticity and visual grading parameters. Constr Build Mater 2022;322:126512. https://doi.org/10.1016/j.conbuildmat.2022.126512.
- [41] Oliveira FGR de, Campos JAO de, Sales A. Ultrasonic Measurements In Brazilian Hardwood. Mater Res 2002;5:51–5. https://doi.org/10.1590/s1516-14392002000100009.
- [42] NSA. SNI 1727 Minimum design load and related criteria. National Standardization Agency; 2020.
- [43] NSA. SNI 1726 Procedures for earthquake resilience design for building and non-building structures. National Standardization Agency; 2019.
- [44] Lingeshwaran N, Koushik S, Reddy TMK, Preethi P. Comparative analysis on asymmetrical and symmetrical structures subjected to seismic load. Mater Sci 2021;45:6471–5. https://doi.org/https://doi.org/10.1016/j.matpr.2020.11.340.